Multidentate Catechol-Based Polyethylene Glycol Oligomers Provide Enhanced Stability and Biocompatibility to Iron Oxide Nanoparticles

Hyon Bin Na,[†] Goutam Palui,[†] Jens T. Rosenberg,[‡,§] Xin Ji,[†] Samuel C. Grant,[‡,§] and Hedi Mattoussi[†,*]

[†]Department of Chemistry and Biochemistry, Florida State University, Tallahassee, Florida 32306, United States, [‡]Chemical and Biomedical Engineering, Florida State University, Tallahassee, Florida 32310, United States, and [§]National High Magnetic Field Laboratory, CIMAR, Tallahassee, Florida 32310, United States

ABSTRACT We have designed, prepared, and tested a new set of multidentate catechol- and polyethylene glycol (PEG)-derivatized oligomers, OligoPEG-Dopa, as ligands that exhibit strong affinity to iron oxide nanocrystals. The ligands consist of a short poly(acrylic acid) backbone laterally appended with several catechol anchoring groups and several terminally functionalized PEG moieties to promote affinity to aqueous media and to allow further coupling to target molecules (bio and others). These multicoordinating PEGylated oligomers were prepared using a relatively simple chemical strategy based on *N,N′*-dicyclohexylcarbodiimide (DCC) and *N*-(3-dimethylaminopropyl)-*N′*-ethylcarbodiimide (EDC) condensation. The ability of these catechol-functionalized oligomers to impart long-term colloidal stability to the nanoparticles is compared to other control ligands, namely, oligomers presenting several carboxyl groups and monodentate ligands presenting either one catechol or one carboxyl group. We found that the OligoPEG-Dopa ligands provide rapid ligand exchange, and the resulting nanoparticles exhibit greatly enhanced colloidal stability over a broad pH range and in the presence of excess electrolytes; stability is notably improved compared to non-catechol presenting molecular or oligomer ligands. By inserting controllable fractions of azide-terminated PEG moieties, the nanoparticles (NPs) become reactive to complementary functionalities *via* azide—alkyne cycloaddition (Click), which opens up the possibility of biological targeting of such stable NPs. In particular, we tested the Click coupling of azide-functionalized nanoparticles to an alkyne-modified dye. We also measured the MRI T_2 contrast of the OligoPEG-capped Fe_3O_4 nanoparticles and applied MTT (3-(4,5-dimethylthiazol-2-yl)-2,5-diphenyltetrazolium bromide) assay to test the potential cytotoxicity of these NPs to live cells; we found no measurable toxicity to live cells.

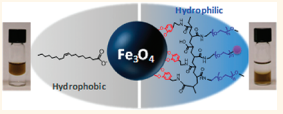

KEYWORDS: iron oxide nanocrystals · synthesis · biocompatibility · surface functionalization · colloidal stability · MRI contrast · cytotoxicity

In the last two decades, a variety of inorganic nanocrystals have been designed, synthesized, and characterized, with the ultimate goals of developing a fundamental understanding of some of their unique chemical, physical, and optical properties while exploiting the potential they offer in applications ranging from electronic devices to biology.[1−7] Their properties often exhibit size and composition dependence and are not shared by their bulk parents or at the molecular scale.[4−7] These unique and controllable properties have permitted researchers across different fields to overcome some of the limitations encountered by conventional (bulk and such) materials for expanding old and developing new technologies. Among these nanostructured materials, pure and metal-doped iron oxide nanocrystals constitute one of the most exciting platforms due to their size- and composition-dependent magnetic properties. They have generated a great deal of interest for use as magnetic resonance imaging (MRI) contrast agents, in magnetic guidance and/or separation, and as biological platforms for intracellular imaging.[7−10] In the early developments (late 1980s), large size superparamagnetic iron oxide nanoparticles (SPIO, with dimensions ≥50 nm) containing several Fe_3O_4 nanocrystals were developed as *in vivo* T_2 MRI contrast agents.[9] More recently, and thanks to some remarkable improvements in the synthesis of high-quality nanocrystals using high-temperature growth methods, preparation of several iron-oxide-based nanocrystals with demonstrated control over size- and composition-dependent magnetic properties have been reported.[11−13] This control has intensified interest in further enhancing the contrast efficiency and understanding the biological distribution of these materials inside organisms.[13,14] However, issues of biological targeting, biodistribution, and *in vivo* toxicity of nanomaterials in general greatly depend on the stability of such nanocrystals

* Address correspondence to mattoussi@chem.fsu.edu.

Received for review September 29, 2011 and accepted December 16, 2011.

Published online December 16, 2011
10.1021/nn203735b

in complex biological media, their biocompatibility, and hydrodynamic dimensions. These properties are directly controlled by one's ability to interface them effectively and reproducibly with biological systems.

A nanoparticle platform with great potential for use in biomedical applications needs to satisfy a few key requirements: (1) The surface coating of the nanoparticle must promote biocompatibility and reduce nonspecific interactions while maintaining an overall compact size. (2) The nanoparticle must exhibit long-term stability over a broad pH range, in the presence of high concentrations of electrolytes and in biological (protein-rich) media. (3) There must be effective and controllable surface functionalization, which permits one to control the number and nature of biomolecules attached to a nanoparticle, thus facilitating the use of these materials in applications such as targeting, sensing, and imaging.

Most effective synthetic strategies that provide high-quality magnetic nanocrystals are based on high temperature reaction of organometallic precursors. They provide nanocrystals that are dispersible mainly in hydrophobic solutions, *i.e.*, water-immiscible nanoparticles. Thus, additional processing using surface ligand exchange or encapsulation within phospholipid micelles or block copolymers is required to transfer these materials to buffer media and to impart biocompatibility. For instance, cap exchange with bifunctional hydrophilic ligands is simple to implement and can produce compact hydrophilic platforms.[13−18] Nonetheless, these strategies often rely on the use of commercially available but ineffective simple ligands or large mass block copolymers. These approaches provide nanoparticles with limited long-term stability and/or substantially increased hydrodynamic size. It has recently been demonstrated that catechol derivatives such as the neurotransmitter dopamine and L-3,4-dihydroxyphenylalanine (L-Dopa), a precursor to dopamine that is also used as a component of adhesives generated by marine mussels, exhibit strong affinity to metal oxide nanocrystals.[16,19,20] Several recent studies have reported that catechol-appended single chain PEGs provide effective capping ligands for iron oxide nanocrystals and permit their transfer to aqueous media. Catechol-PEG-capped iron oxide nanoparticles also have been used in cellular labeling and targeted MR imaging studies.[17,18,21−23] It has been shown that ligands presenting multiple anchoring groups (increased coordination to the inorganic surface) can substantially enhance the affinity of the ligands to the nanocrystal surfaces, which produces hydrophilic nanocrystals that are stable in complex biological conditions. For example, we have demonstrated the benefits of this strategy for the dispersion of luminescent quantum dots and gold nanoparticles in buffer media.[24−26] Other groups have explored its effectiveness for capping additional semiconducting and magnetic nanoparticles.[27−29] In one approach, Tremel and co-workers tested the use of a polymer chain made of polyinosinic−polycytidyl acid presenting laterally a few dopamines, alkylamines, and a dye to cap TiO_2 and γ-Fe_2O_3 nanoparticles.[30−33] In this scheme, the water solubility relied on the presence of a few nonactivated carboxyl groups on the polymer chain, that is, electrostatically driven affinity to aqueous solutions. They further tested the ability of these nanoparticles coupled to oligonucleotides to image live cells.[32,33]

In this study, we build on the above developments and report the design, preparation, and characterization of a new set of catechol-derivatized and polyethylene-glycol-appended oligomeric ligands. These ligands consist of a short oligomer backbone made of poly(acrylic acid) (PAA) that is laterally appended with several poly(ethylene glycol) (PEG) moieties and two types of metal-coordinating groups: (1) catechol groups, and (2) carboxylic acid groups, providing OligoPEG-Dopa and OligoPEG-COOH, respectively. The PEG and catechol moieties are randomly grafted onto the PAA backbone using *N*,*N*′-dicyclohexylcarbodiimide (DCC) and *N*-(3-dimethylaminopropyl)-*N*′-ethylcarbodiimide (EDC) coupling, respectively. Multigram quantities of purified oligomer ligands can be made using this route. Monocatechol and mono-COOH-appended short PEGs were prepared and used as control. We found that rapid and facile ligand exchange of hydrophobic iron oxide nanoparticles with these ligands takes place, and that the oligomers exhibit strong affinity to iron oxide nanocrystals, as dispersions of nanoparticles that are stable over a broad range of pH values and electrolyte conditions have been prepared and tested. When the PEG moieties are appended with terminal reactive groups, controllable coupling to biological receptors can be realized. For instance, we have used Cu-catalyzed Click to attach alkyne-modified dyes to azide-functionalized OligoPEG-Dopa-Fe_3O_4 nanoparticles (NPs). This modification can permit further use of the hydrophilic nanoparticles in custom-designed bio-oriented applications. In addition, we carried out MRI relaxometry experiments using these OligoPEG-Dopa-capped Fe_3O_4 NPs and found that the contrast depends on size and concentration of the NPs. Finally, we tested the effectiveness of our surface coating scheme to reduce cytotoxicity to live cells using MTT (3-(4,5-dimethylthiazol-2-yl)-2,5-diphenyltetrazolium bromide) assay.

RESULTS AND DISCUSSION

The oligomer design builds on previous experience and results reported in the literature, which have shown that appending multi-thiol coordinating groups at the end of a PEGylated moiety produces a dramatic enhancement in the ligand affinity to quantum dots

(QDs) and gold nanoparticles (Au NPs) alike. Those studies have also proven that inserting PEG segments in the ligand structures allows for substantially improved nanocrystal stability in biological media.[24−26] For example, our group has developed PEG-based ligands appended with two thioctic acid (TA) or two dihydrolipoic acid (DHLA) anchoring groups, where the Michael addition was used to create a branch point allowing for the attachment of two TA onto a single PEG.[26] These ligands provided QDs and Au NPs with greatly enhanced stability in buffer media at extreme pH values. Here, we wanted to expand on those rationales and develop a multidentate ligand with strong affinity to iron oxide nanocrystals. We have taken a slightly different approach, though, where a short PAA ($M_w \sim 1800$ or an index of polymerization of ~25) was chosen as a platform/backbone to graft multiple anchoring groups along with multiple PEG moieties within the same structure. This design maintains a relatively low molecular weight and small size of the ligand, while accommodating several anchoring groups and several PEG moieties. We tested OligoPEG with two types of anchoring groups: (1) The native carboxyl groups present on the poly(acrylic acid) oligomer; here a fraction of the carboxylic acid groups was reacted with amine-appended PEG, providing a ligand presenting several carboxyl groups and several PEG moieties, OligoPEG-COOH (compound **1**). (2) Several dopamines and amine-terminated PEGs were grafted onto the PAA, producing an oligomer that presents several catechol anchoring groups together with multiple PEG moieties, OligoPEG-Dopa (compound **2**). We also prepared and tested two molecular scale PEG-appended ligands, a mono-PEG-Dopa (compound **3**) and a mono-PEG-COOH (compound **4**). Here, we used OligoPEG-COOH, mono-PEG-Dopa, and mono-PEG-COOH as control ligands to which the data on the OligoPEG-Dopa were compared. This allowed us to test the effects of coordination number as well as the nature of the anchoring group used on the cap exchange and on the quality of the resulting Fe_3O_4 nanoparticles.

Figure 1 provides a schematic depiction of the synthetic steps involved in the preparation of the carboxyl- and catechol-PEG-derivatized oligomers. We used commercial PAA, along with molecular scale bifunctional PEG moieties, which we have described in previous reports.[24,25] For the OligoPEG-COOH ligand (compound **1**), a fraction of the carboxylic acids along the PAA backbone was reacted (*via* DCC coupling in THF) with NH_2-PEG-OCH_3. Characterization of the oligomer ligand using ^{1}H NMR spectroscopy (in DMSO-d_6) showed that multiple PEG moieties were indeed coupled to the PAA, as indicated by the appearance of a new strong broad peak at 3.26−3.64 ppm (attributed to PEG segments) and a second sharp peak at 3.23 ppm attributed to OCH_3 groups; the weak broad peaks at 1.1−2.3 ppm are ascribed to PAA (Figure 2a). We should note that the exact location of these peaks depends on the solvent used. For example, a peak at 3.38 ppm was measured for this methoxy group in $CDCl_3$.[24] FT-IR analysis further confirmed the presence of amide bonds linking the PEG moieties to PAA with bands at 1645 and 1531 cm^{-1} (see the Supporting Information Figure S1). In a typical experiment, the degree of grafting was estimated from the ^{1}H NMR spectrum by comparing the relative integrations of the α-hydrogen peak from the acrylic acid repeat units of PAA (δ = 1.86−2.23, 25H) and the three protons in the lateral methoxy group of PEG-OCH_3 (δ = 3.23, 38.8H); we measured ~13 PEG moieties per PAA chain.

To prepare azide-functionalized OligoPEG-COOH (*e.g.*, compound **1**-**1**), a mixture of OCH_3- and N_3-terminated PEG-NH_2 moieties was used during the DCC coupling reaction. By varying the relative amounts (fractions) of azide-PEG and OCH_3-PEG moieties, one can control the number of azide groups per oligomer. In this report, we detailed the preparation and characterization of an azide-functionalized OligoPEG-COOH with a nominal azide-to-methoxy ratio of 1:3 (or 25% azide-PEG). The azide signature manifests as a triplet peak at 3.39 ppm in the ^{1}H NMR spectrum; additionally, a new vibration band at 2108 cm^{-1} is measured in the FT-IR spectrum (Figure 2b; see also the Supporting Information Figures S2).

For the OligoPEG-Dopa ligands (compounds **2** and **2**-**1**), the synthesis was carried out in two steps: (1) A fraction of the carboxyl groups along the PAA backbone was reacted (*via* DCC in the presence of DMAP in THF) with either NH_2-PEG-OCH_3 or a mixture of NH_2-PEG-OCH_3 and NH_2-PEG-N_3, as done above for the OligoPEG-COOH (compounds **1** and **1**-**1**). (2) After purification, the rest of the carboxyl groups along the PEGylated oligomer intermediate were reacted (*via* EDC condensation) with dopamine. We found that the use of EDC condensation (instead of DCC) allowed not only a more efficient coupling between the carboxylic acids along the PAA (OligoPEG-COOH) and dopamine but also facile removal of the byproducts and unreacted precursors by dialysis. ^{1}H NMR analysis confirmed that catechol groups, PEG moieties, and methoxy groups are present in the oligomer. In particular, a multiplet at 6.32−6.78 ppm (catechol protons), a strong peak at 3.26−3.64 ppm (due to PEG), and a sharp peak at 3.23 ppm (due to methoxy) were measured in the NMR spectra (see Figure 2). The degree of grafting was estimated to be 6.2 catechols per chain (or oligomer), derived from comparing the relative integrations of the 25 α-hydrogens from the acrylic acid repeat unit of PAA (δ = 1.86−2.23, 25H) and the three protons per catechol (δ = 6.32−6.78, 18.5H total). In addition, FT-IR data analysis for the OligoPEG-Dopa (compound **2**) showed a sizable decrease in the signature of carboxyl groups at 1722 cm^{-1}, which

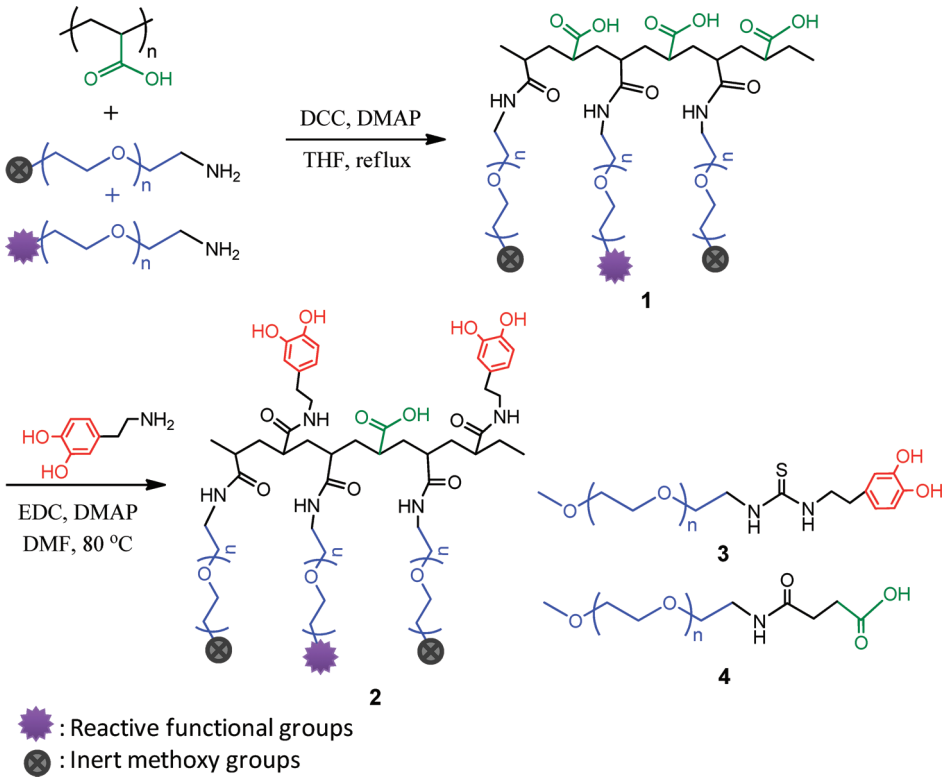

Figure 1. (Top) Preparation of OligoPEG-COOH ligand (compound 1) was carried out in THF and relied on DCC coupling; either pure H_3CO-PEG-NH_2 or a mixture of H_3CO-PEG-NH_2 and N_3-PEG-NH_2 was used. (Bottom left) Synthesis of OligoPEG-Dopa (compound 2) was carried out in two successive steps. In the first, H_3CO-PEG-NH_2 or a mixture of H_3CO-PEG-NH_2/N_3-PEG-NH_2 was grafted onto the PAA backbone, as done above for compound 1. Dopamines were then coupled to the unreacted carboxyl groups along the PAA using EDC to provide OligoPEG-Dopa ligand. (Bottom right) Structure of mono-PEG-Dopa (compound 3) and mono-PEG-COOH (compound 4) are provided.

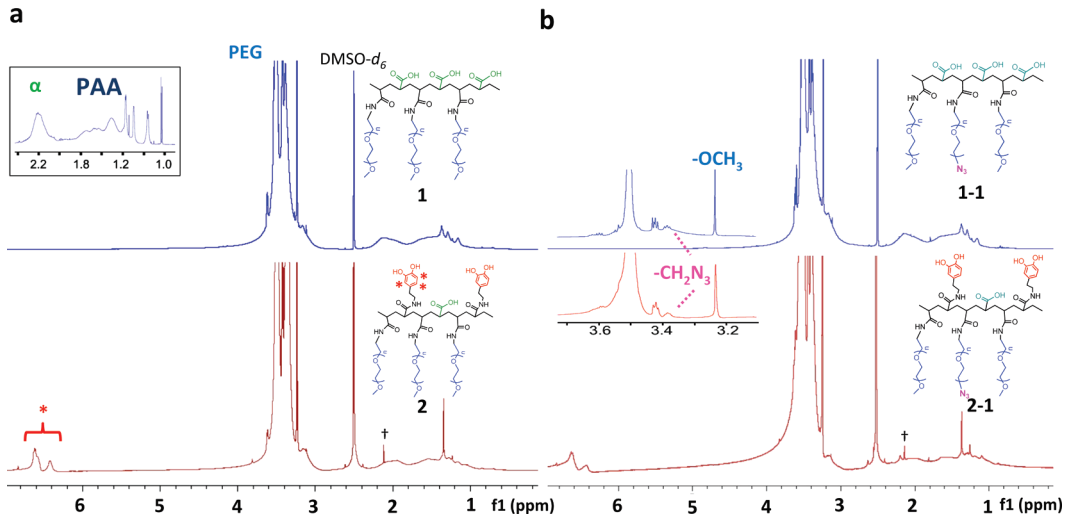

Figure 2. (a) Spectra of OligoPEG-COOH (compound 1) and OligoPEG-Dopa (compound 2) measured in DMSO-d_6. The signature of PEG around 3.26−3.64 ppm and the singlet peak from the protons of methoxy at 3.23 ppm are dominant in spectra. Multiplet peaks around 1.86−2.23 ppm (α) and at 6.32−6.78 ppm (*) were ascribed to the α-hydrogens of PAA and the protons in the catechols, respectively. Inset shows the ^{1}H NMR spectrum of PAA. (b) Spectra of azide-functionalized OligoPEG-COOH (compound 1-1) and azide-functionalized OligoPEG-Dopa (compound 2-1) measured in DMSO-d_6. The signature of azide (−CH_2N_3) at 3.39 ppm and the singlet peak from the protons of methoxy at 3.23 ppm are present in both spectra (inset). The peak signatures of PEG, the α-hydrogens of PAA, and the protons in the catechols are identical for OligoPEG-COOH and OligoPEG-Dopa. The peak in the spectra at 2.1 ppm, marked by †, is attributed to acetone.

provides further inference that catechol groups have been grafted onto the PAA backbone during this reaction step (see the Supporting Information Figures S1 and S2).

Additional, though indirect, proof for the presence of catechol groups in the OligoPEG-Dopa ligand structure relied on UV−vis absorption, for which a clear pH-dependent change in the absorption spectra of compound **2** was measured. In particular, we measured a progressive increase coupled with broadening of the peak at 280 nm for compound **2** as the pH of the solution was increased. The most pronounced changes were measured at pH ≥ 9, with equilibrium usually reached after 90 min. This change in absorption is similar to that measured for the mono-PEG-Dopa ligand (compound **3**); see the Supporting Information. This change is a characteristic signature of the catechol group in the presence of oxygen when the solution pH is increased.

We found that ligand exchange of Fe_3O_4 nanoparticles (capped with the native oleic acid) can be carried out using the three sets of ligands, namely, mono-PEG-Dopa, OligoPEG-COOH, and OligoPEG-Dopa. However, we observed substantial differences between the various ligands in the ease of implementing the cap exchange procedure and in the long term stability to changes in pH and to added electrolytes. While cap exchange with the OligoPEG-Dopa and even the mono-PEG-Dopa was rapid and required only incubation at room temperature, cap exchange with OligoPEG-COOH ligand required heating at ∼70 °C. In comparison, mono-PEG-COOH (compound **4**) could not stabilize iron oxide NPs even with longer incubation times and heating at ∼70 °C. This reflects the inherent weak coordination of a single COOH group (compared to a single catechol) to iron oxide surfaces. TEM images of nanoparticles cap exchanged with OligoPEG-Dopa (compound **2**), shown in Figure 3, indicate that the integrity of the NPs was conserved, with no change in the overall size or shape; this confirms that the new ligands did not induce any damage or leaching of metal ions off the NP surfaces. In addition, dynamic light scattering (DLS) measurements applied to the larger size nanoparticles ($R_0 \sim 11$ or 22 nm diameter from TEM) showed that water dispersions of the OligoPEG-capped iron oxide nanoparticles exhibit no sign of aggregation. Furthermore, the hydrodynamic size measured for the hydrophilic nanocrystals was only slightly larger than the one measured for their hydrophobic (oleic-acid-capped) counterparts; R_H measured for oleic-acid-capped NPs in hexane is ≅16 nm, and it slightly increased to ≅19 nm for OligoPEG-Dopa-NPs in deionized water. This confirms the ability of our ligand design to provide compact and aggregation-free dispersions of iron oxide nanoparticles; additional details are provided in the Supporting Information.

Side-by-side comparison of the stability of iron oxide NPs capped with the PEGylated oligomers to pH changes showed that, while both compounds provided dispersions that were stable over the short-term, only the OligoPEG-Dopa provided well-dispersed NPs over the full range of pH values. For instance, OligoPEG-COOH-NPs slowly became turbid and precipitated after ∼5 weeks of storage, but at pH 11 or higher, precipitation occurred after 1 day. Conversely, NPs cap-exchanged with mono-PEG-Dopa exhibited limited stability, as precipitation took place after 1 day at pH 4 and after 35 days at basic pH 11 or higher (see Figure 4a). Stability of NP dispersions to excess electrolytes (namely, 1 M NaCl) exhibited a similar trend. The images shown in Figure 4b indicate that OligoPEG-Dopa ligand produces more stable NP dispersions than OligoPEG-COOH and mono-PEG-Dopa, as NPs capped with compound **1** precipitated after 1 month of storage and those capped with compound **3** precipitated after 10 days. In comparison, NPs capped with compound **2** stayed stable for at least 2 months. When dispersed in DI water, NPs capped with compound **2** stayed stable for longer times, at least 6 months. In control experiments, we tested the stability of the pure ligands and found that both sets, OligoPEG-Dopa and OligoPEG-COOH, stayed dispersed (with no sign of turbidity build up) in buffers over a broad range of pH (pH 4−12) and in the presence of added excess salt. A slight change in the color of OligoPEG-Dopa solutions was observed at higher pH values; this is attributed to oxidation of dopamines to quinones at basic pH values. We also monitored the stability of iron oxide NPs capped with the new ligands in cell culture media (using RPMI-1640 media, Sigma Aldrich). We found that NPs stabilized with OligoPEG-Dopa, OligoPEG-COOH, and mono-PEG-Dopa were equally stable in the media for a short period of storage (∼2−3 weeks). However, only dispersions OligoPEG-Dopa-NPs stayed stable for at least 1 month (duration of the test), while the NPs capped with mono-PEG-Dopa and OligoPEG-COOH started showing signs of slow aggregation buildup. Additional details are provided in the Supporting Information.

Cumulatively, these tests confirm that individually a catechol group exhibits much stronger affinity to iron oxide than a carboxyl group, though long-term stability provided by both ligands is poor. They also clearly prove that ligands presenting multiple carboxyl groups or multiple catechols exhibit enhanced binding to the nanoparticle surface; sizable differences between the two types of oligomers exist nonetheless. In particular, we found that the multi-catechol presenting ligand (compound **2**) imparts the highest stability against changes in the solution pH and to added NaCl. This supports prior findings for which the benefits of multi-coordinating ligands and their ability to impart better colloidal stability to Au NPs and QDs (due to enhanced binding affinity) has been documented by us and others.[24−27] However, reports on the hydrophilic stabilization of metal oxide NPs (such as Fe_3O_4) were rather limited.[13,21,27,28] Most promising results were

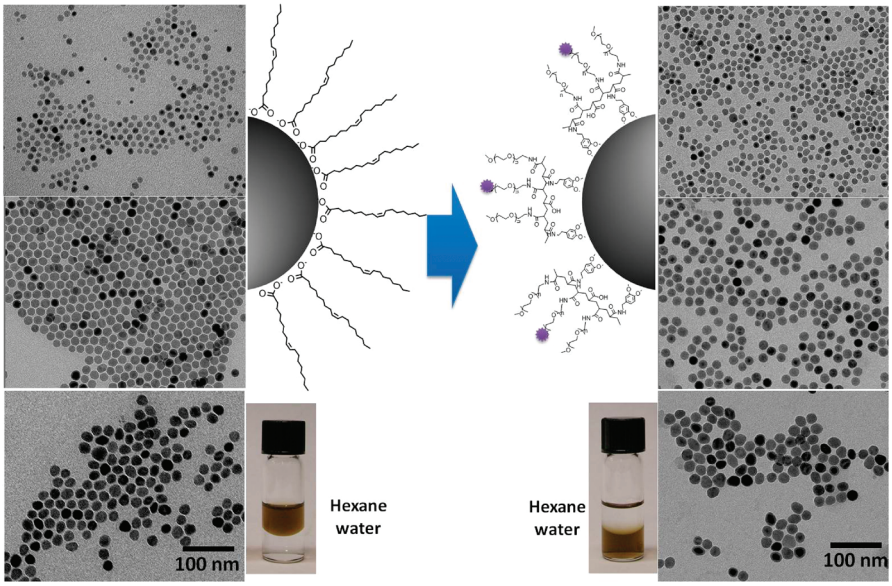

Figure 3. TEM images of Fe_3O_4 NPs with 11, 17, and 23 nm core size before (left) and after (right) ligand exchange with OligoPEG-Dopa. Schematic representation of the NP with the corresponding surface cap along with images of the organic and aqueous dispersions are shown.

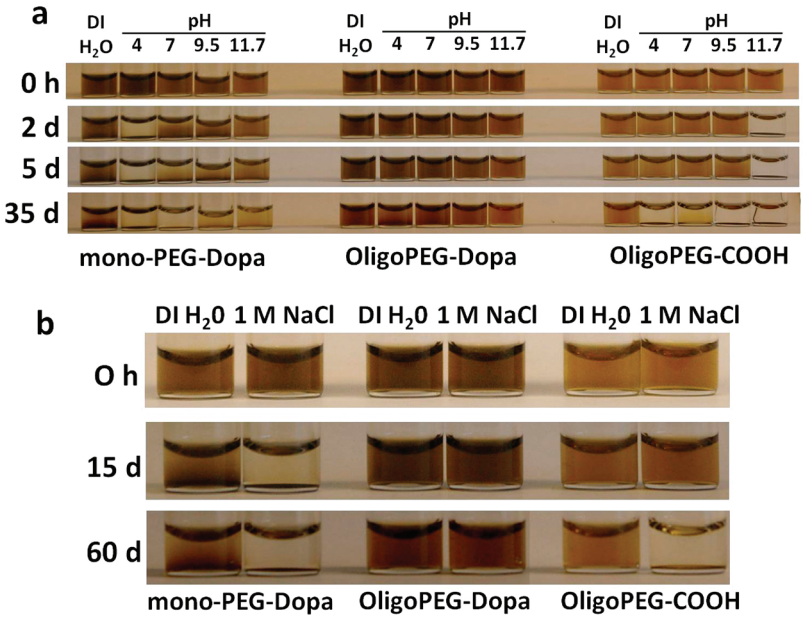

Figure 4. (a) Stability test of Fe_3O_4 NP dispersions in various pH buffers. Shown are mono-PEG-Dopa-stabilized NPs (left), OligoPEG-Dopa-stabilized NPs (middle), and OligoPEG-COOH-stabilized NPs (right). (b) Stability of Fe_3O_4 NP dispersion in 1 M NaCl. Shown are mono-PEG-Dopa-NPs (left), OligoPEG-Dopa-NPs (middle), and OligoPEG-COOH-NPs (right).

obtained mainly *via* encapsulation within large molecular weight block copolymers or silica shell, albeit with the sizable increase in the NP hydrodynamic size.[34−36] Our present ligand offers a promising platform for substantially improving the stability of such magnetic nanoparticles in variety of biologically relevant conditions, including acidic, basic, and electrolyte- and protein-rich media. We carried out three additional and independent tests on the new set of nanoparticles with direct implications in biology.

(1) We first tested the ability to conjugate the newly designed OligoPEG-NPs to alkyne-modified fluorescent dye using copper(I)-catalyzed azide−alkyne cycloaddition (CuAAC or Click) reaction. Fe_3O_4 NPs cap-exchanged with compound **2**-**1** were designed to present a few azide-terminated PEG moieties on their surfaces, making them potentially compatible with Click reaction. Azide−alkyne cycloaddition as a coupling strategy has generated a tremendous

interest and activity because of its efficiency, high chemoselectivity, and reduced cross-reactivity.[37−40] It is also compatible with a wide range of solvents and pH values. Click offers a good alternative to other more conventional reaction schemes that often rely on the reactivity of amide, ester, or thioether with naturally abundant carboxyl, amine, and thiol groups. Their abundance, however, can induce high levels of nonspecific and unintended conjugation of proteins and peptides.[40−42] To demonstrate the compatibility of our azide-functionalized OligoPEG-Dopa-NPs with this coupling route, we reacted the NPs with an alkyne-modified rhodamine B dye (see scheme in Figure 5a and Experimental Section). The dye-conjugated NPs were characterized using absorption and fluorescence measurements. Figure 5b shows the absorption and fluorescence spectra of the dye-reacted NP dispersions following purification. Both spectra indicate the presence of bound rhodamine B onto the NPs. In particular, there is an additional absorption peak at ~566 nm and a pronounced fluorescence signal characteristic of the rhodamine B dye at 577 nm; the deconvoluted dye contribution to the absorption spectrum is shown in the inset in Figure 5b. These optical signatures are characteristic of the rhodamine B dye, clearly confirming that Click-driven coupling between the azide-functionalized NPs and alkyne-rhodamine B has taken place. The absorption and fluorescence peaks of the NP-attached dye exhibit a small red shift compared to the dye alone; such shifts are often observed when dyes are attached to proteins and peptides. From the absorption data and using the extinction coefficient for rhodamine B (87 000 M^{-1} cm^{-1} at 554 nm, peak), we estimate that there are ~82 dyes per Fe_3O_4 nanoparticle. Though preliminary, this result clearly proves the potentials of our ligand design applied to magnetic NPs and could allow for developing a multimodal imaging agent based on MR contrast.

(2) In the second test, we evaluated the MRI contrast signature of Fe_3O_4 NPs capped with OligoPEG-Dopa ligands (iron oxide NPs have been tested as efficient T_2 MRI contrast agents). Three different size NPs (11, 17, and 23 nm diameter as estimated from TEM) stabilized with compound **2** were prepared and dispersed in buffer solutions. T_1, T_2, and T_2* signals were collected and used to extract estimates for r_1, r_2, and r_2* relaxavities. Figure 5c shows the T_2-weighted spin−echo images of the different NPs with varying dilutions, along with the corresponding T_2*-weighted gradient recalled echo images. A strong enhancement in the T_2 and T_2* contrast signals with nanoparticle concentration and size was measured. We also measured a consistent trend in the size dependence of relaxivity, with r_2 = 181, 234, and 254 mM^{-1} s^{-1} for 11, 17, and 23 nm NPs, respectively. (Additional information is provided in the Supporting Information.) We would like to stress that the measured relaxivity r_2 values for our hydrophilic Fe_3O_4 NPs are well in excess of those reported for commercial clinical agents. For example, some of the highest values reported for those agents (B_0 = 0.47 T) are Feridex/Endorem (r_2 = 160 mM^{-1} s^{-1}), Resovist (r_2 = 151 mM^{-1} s^{-1}), and Sinerem (r_2 = 160 mM^{-1} s^{-1}).[43,44]

(3) Stability, biocompatibility, and reduced interference with the biological functions of cells and animal functions of these magnetic nanoprobes is critical for use in applications, such as *in vitro* and *in vivo* imaging and sensing. Our OligoPEGs present a high number of biocompatible PEG moieties, which makes them highly suitable for biological environments. We assessed the cytotoxicity of the OligoPEG-Dopa-stabilized Fe_3O_4 nanoparticles (11 nm size) using MTT (3-(4,5-dimethylthiazol-2-yl)-2,5-diphenyltetrazolium bromide) assay on a rat microglia cell line (Bv2). The final concentration of Fe_3O_4 nanoparticles in the cell media was varied between 0.0625 and 2 mM (of equivalent Fe); further experimental details are provided in the Supporting Information. Figure 5d shows that cell viability was largely unaffected by the presence of the NPs. The MTT assay proves that the present set of nanoparticles essentially has no measurable toxicity to the cells, further supporting our rationale that these multidentate PEG-rich oligomers should provide added biological compatibility to the magnetic nanoparticles, thus enhancing their potential utility in biomedical applications.

We now would like to provide a comparison between our OligoPEG design and that previously reported by Tremel and co-workers.[30−33] The two designs rely on the use of dopamine anchors for capping iron oxide nanocrystals and combine that with the use of reactive groups for further coupling to target molecules. There are a few important differences, nonetheless. In their strategy, they used a full size polymer cap, where transfer of the nanoparticles to water relied on the availability of carboxyl groups along the backbone. This inevitably produces larger size hydrophilic nanoparticles combined with potentially pH-dependent solubility as carboxyl groups will eventually protonate in acidic conditions. Our OligoPEG ligand design has improved on those ideas by

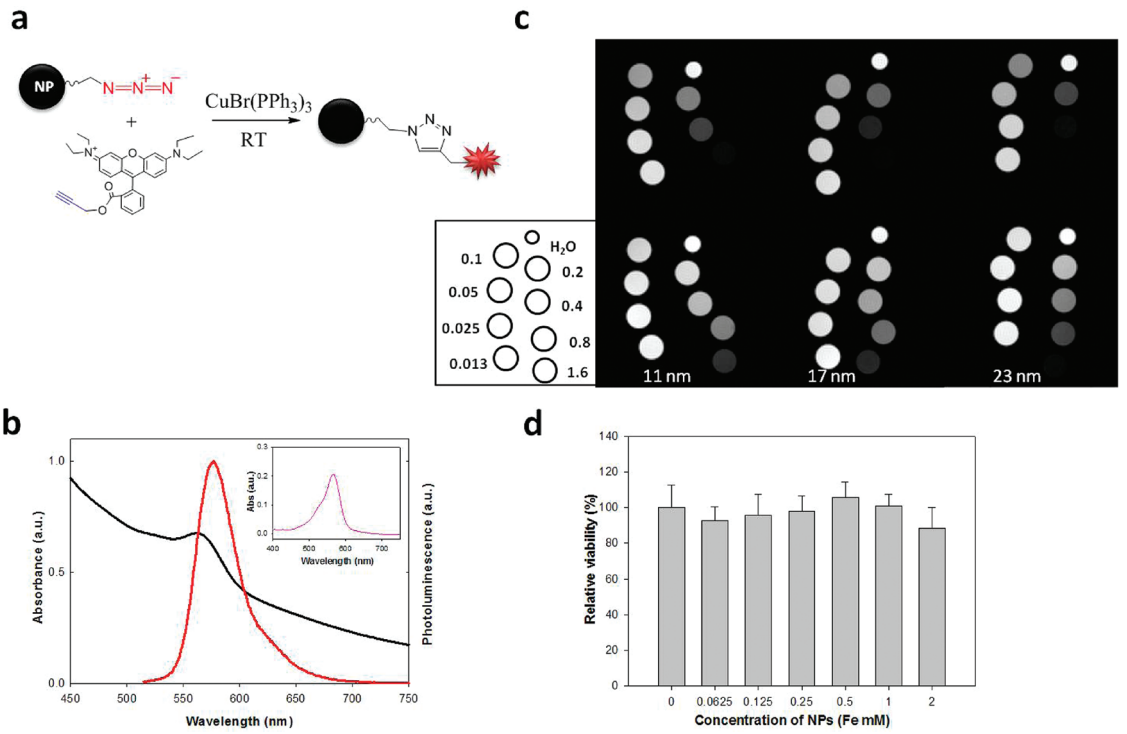

Figure 5. (a) CuAAC conjugation of alkyne-functionalized dyes to azide-functionalized iron oxide NPs. (b) Absorption (black) and fluorescence (red, λ_{ex} = 500 nm) spectra after rhodamine B conjugation to azide-functionalized OligoPEG-Dopa-NPs. Inset shows the deconvoluted spectrum of rhodamine B. (c) Top row: T_2-weighted spin−echo images (TE/TR = 16/5000 ms) of the different size nanoparticles with increased dilutions as shown in the inset. Bottom row: T_2*-weighted gradient recalled echo images (TE/TR = 3/5000 ms); the corresponding iron concentrations (in mM) in each capsule are shown in the drawn sketch below. (d) Plot of the relative viability of Bv2 cells for increasing concentration of OligoPEG-Dopa-stabilized Fe_3O_4 nanoparticles performed using MTT assay.

starting from a short chain (~25 monomers) and introducing controllable numbers of catechol anchoring groups, PEGylated moieties, and terminally reactive functions, all in the same cap while using small size PEG segments. This produces small molecular weight ligands.

The present design also improves on our earlier approaches using TA-, DHLA-, bis(TA)-, and bis(DHLA)-appended methoxy-PEG ligands to cap QDs.[24−26] The use of oligomers has permitted the facile combination of anchoring groups, reactive groups, and PEGylated moieties all in the same ligand(s). Furthermore, the use of a short backbone with small molecular weight (PAA with M_w = 1800) still guarantees compact capping layer. Encapsulation within phospholipid micelles and block copolymers, also commonly employed strategies, tend to provide rather large size nanoparticles and/or limited long-term stability under biologically relevant conditions. Some of the polymer encapsulation strategies also rely on electrostatically induced solubility, where carboxyl and other chargeable groups are used.[34,45−47]

CONCLUSION

We described the use of newly designed multicatechol and PEG-appended oligomers to cap iron oxide nanoparticles and transfer them to buffer media. Our ligands were prepared by laterally grafting several PEG moieties and several catechol groups onto a poly(acrylic acid) short chain. In this design, the intrinsic ligand structure, including the density of anchoring groups, the size of PEG, and the type of end reactive groups can be controlled, all while maintaining a compact size. Cap exchange with these oligomers was rapid and provided iron oxide NPs that are stable for at least 60 days in the presence of large excess of added salts and over a broad range of pH values, from pH 4 to pH 11. Colloidal stability is vastly improved compared to other lower coordination ligands such as mono-PEG-catechol or oligomers presenting weaker coordinating COOH groups. We also showed that controllable fractions of azides can be introduced into the oligomer ligand, producing NPs that are reactive with complementary functionalities. In particular, we demonstrated the ability to couple azide-functionalized NPs to an alkyne-modified dye, which opens up the possibility of biological targeting of these NPs. We also measured the MRI contrast properties of these OligoPEG-capped Fe_3O_4 nanoparticles and found that they exhibit strong T_2 contrast enhancement with dependence on the size of the nanocrystals. Preliminary MTT assay using these OligoPEG-NPs indicated no measurable toxicity of the NPs to live cells. We believe that this approach can be expanded to prepare other

types of functionalized oligomers with tailor-designed anchoring groups and reactive groups, which will allow the hydrophilic transfer and coupling of a variety of inorganic nanocrystals.

EXPERIMENTAL SECTION

Synthesis of OligoPEG-COOH (Compound 1). Four grams of poly(acrylic acid) (PAA, M_w = 1800, 2.22 mmol) was dispersed in 100 mL of tetrahydrofuran (THF) in a 250 mL round-bottom flask and cooled to 0 °C using an ice-bath with stirring. Then, 4.59 g of *N*,*N*′-dicyclohexylcarbodiimide (DCC, 22.22 mmol) was added, and the mixture was stirred for 30 min under N_2. Then, 0.54 g of 4-(*N*,*N*-dimethylamino)pyridine (DMAP, 4.44 mmol) and 16.34 g of H_2N-PEG750-OCH_3 (22.22 mmol) were added, and the mixture was left refluxing for 2 days at ~70 °C. The reaction mixture was filtered using a filter funnel and the solvent evaporated. Deionized water (100 mL) containing 4 g of KOH was added to the residue, and the mixture was left stirring overnight, filtered, washed with ethyl acetate, and acidified using 1 N HCl solution to a pH 4. Chloroform was added to the aqueous solution to extract the product (3 times 100 mL each). The organic layers were combined dried over Na_2SO_4 and filtered, and the solvent evaporated under vacuum to yield the crude product, which was further purified on a silica gel column using chloroform as the eluent.

Synthesis of Azide-Functionalized OligoPEG-COOH (Compound 1-1). In a 250 mL round-bottom flask, 2.0 g of PAA (M_w 1800, 1.11 mmol) was dispersed in 50 mL of THF and cooled to 0 °C using an ice-bath with stirring. Then, 2.29 g of DCC (11.11 mmol) was added, and the mixture was stirred for 30 min under N_2. DMAP (0.27 g, 2.22 mmol), H_2N-PEG750-OCH_3 (6.13 g, 8.33 mmol), and H_2N-PEG600-N_3 (1.73 g, 2.78 mmol) were added and the mixture left refluxing at ~70 °C for 2 days. The reaction mixture was filtered, the solvent was evaporated, then 100 mL of deionized water mixed with 2 g of KOH was added to the residue. After overnight stirring, the mixture was filtered then washed with ethyl acetate. The aqueous phase was acidified using 1 N HCl to pH 4, and the product was extracted with chloroform (3 times at 100 mL each). The combined organic layer was dried over Na_2SO_4, filtered, and the solvent evaporated. The product was further purified by silica gel column chromatography using chloroform as the eluent.

Synthesis of OligoPEG-Dopa (Compound 2). In a 100 mL round-bottom flask 320 mg of *N*-(3-dimethylaminopropyl)-*N*′-ethylcarbodiimide hydrochloride (EDC, 1.67 mmol) was dispersed in 10 mL of dimethylformamide (DMF) with equivalent molar amount of triethylamine. One gram of compound **1** (OligoPEG-COOH, 0.11 mmol) was added, and the mixture was cooled to 0 °C using an ice-bath with stirring. In a separate round-bottom flask (50 mL), 475 mg of dopamine hydrochloride (2.50 mmol) was dispersed in 10 mL of dimethylformamide (DMF) with equivalent molar amount of triethylamine and stirred for 30 min at room temperature, then 41 mg of DMAP (0.33 mmol) was added. This dopamine solution was added to the solution containing compound **1**, and the mixture was heated to 80 °C and left stirring for 5 days. After evaporating the solvent, 20 mL of deionized water containing 1 g of KOH was added to the flask, and the mixture was stirred overnight. The mixture was filtered, washed with ethyl acetate, and after neutralization by the addition of 1 N HCl, the mixture was dialyzed using a cellulose ester membrane with M_w cutoff of 1000 Da. The product was reduced with 1% hydrazine in deionized water, further purified *via* two rounds of dialysis and then lyophilized.

Synthesis of Azide-Functionalized OligoPEG-Dopa (Compound 2-1). EDC (218 mg, 1.14 mmol) was dispersed in 5 mL of DMF with equivalent molar amount of triethylamine in a 100 mL round-bottom flask. Then, 0.66 g of azide-functionalized OligoPEG-COOH (compound **1**-**1**, 0.08 mmol) was added, and the mixture was cooled to 0 °C using an ice-bath while stirring. In a separate vial, 324 mg of dopamine hydrochloride (1.71 mmol) was dispersed in 5 mL of DMF with equivalent molar amount of triethylamine, and the mixture was stirred at room temperature. After 30 min, the dopamine solution and 28 mg of DMAP (0.23 mmol) were added to the solution containing EDC and compound **1**-**1**. The mixture was left stirring at 80 °C for 5 days. After evaporating solvent, 10 mL of deionized water containing 0.66 g of KOH was added to the residue and stirred overnight. The solution mixture was filtered and washed with ethyl acetate. After neutralization by addition of 1 N HCl solution, the product was purified by dialysis using cellulose ester membrane (M_w cutoff = 1000 Da). The product was reduced with 1% hydrazine in deionized water, further purified by dialysis, and lyophilized.

Cap Exchange of Iron Oxide Nanopartides. The iron oxide NPs were synthesized using thermal decomposition of Fe-oleate in high-boiling-point solvents, characterized, and processed using procedures developed by Hyeon and co-workers.[12] Here, we briefly describe the procedure used for capping Fe_3O_4 NPs with compound **2** (OligoPEG-Dopa). Five milligrams of iron oxide NPs with varying sizes (11, 17, and 23 nm) dispersed in 0.5 mL of THF was mixed with 25 mg of OligoPEG-Dopa, initially dissolved in 1 mL of ethanol, and stirred overnight at room temperature, resulting in a clear solution. The sample was precipitated using hexane and centrifuged to provide a dark pellet of NPs. The dark pellet was readily dispersed in water, providing a clear solution. The aqueous dispersion was filtered through a 0.2 μm disposable syringe filter (Millipore), then excess free ligands and solubilized oleic acid were removed using 2−3 rounds of filtrations with deionized water (2−3 times) using a centrifugal filtration device (Millipore, M_w cutoff = 100 kDa). Cap exchange with mono-PEG-Dopa followed the same steps as those employed with compound **2**. The cap exchange with OligoPEG-COOH ligand (compound **1**) followed the same procedure, except that the NP/ligand mixture in THF and ethanol required a slight heating to ~70 °C and incubation for longer times. Similar steps were employed for capping the NPs with mono-PEG-COOH.

Dye Conjugation *via* Copper(I)-Catalyzed Azide−Alkyne Cycloaddition. The alkyne-modified rhodamine B (RhB-alk) was synthesized *via* EDC coupling between rhodamine B and propargyl alcohol following the procedure described in ref 40. For NP conjugation, 30 μL of RhB-alk solution (2 mg/mL in DMSO) was mixed with 300 μL of azide-functionalized OligoPEG-Dopa-NPs dispersion (400 nM) in the presence of $CuBr(PPh_3)_3$ and stirred for 1 day at room temperature. After purification by the size exclusion using a PD10 column (GE healthcare) with DI water and filtration through a 0.4 μm disposable syringe filter (Millipore), the eluted solution was characterized using absorption and fluorescence measurements.

Acknowledgment. The authors thank FSU, the National Science Foundation, and Pfizer for financial support. H.B.N. was supported by a fellowship from the National Research Foundation of Korea (D00074). MR experiments and J.T.R. were supported by the American Heart Association (3860040), and conducted at the FAMU-FSU College of Engineering. We thank Joe Schlenoff and Zaki Estephan for assistance with the DLS experiments.

Supporting Information Available: Additional experimental details on sample characterization, stability tests, MRI relaxometry measurements, and cell viability assay. This material is available free of charge *via* the Internet at http://pubs.acs.org.

REFERENCES AND NOTES

1. Murray, C. B.; Kagan, C. R.; Bawendi, M. G. Synthesis and Characterization of Monodisperse Nanocrystals and Close-Packed Nanocrystal Assemblies. *Annu. Rev. Mater. Sci.* **2000**, *30*, 545–610.
2. Park, J.; Joo, J.; Kwon, S. G.; Jang, Y.; Hyeon, T. Synthesis of Monodisperse Spherical Nanocrystals. *Angew. Chem., Int. Ed.* **2007**, *46*, 4630–4660.

3. Kwon, S. G.; Hyeon, T. Colloidal Chemical Synthesis and Formation Kinetics of Uniformly Sized Nanocrystals of Metals, Oxides, and Chalcogenides. *Acc. Chem. Res.* **2008**, *41*, 1696–1709.
4. Klabunde, K. J.; Richards, R. *Nanoscale Materials in Chemistry*, 2nd ed.; Wiley: Hoboken, NJ, 2009.
5. Mattoussi, H.; Cheon, J. *Inorganic Nanoprobes for Biological Sensing and Imaging*; Artech House: Boston, MA, 2009.
6. Klimov, V. I. *Nanocrystal Quantum Dots*, 2nd ed.; CRC Press: Boca Raton, FL, 2010.
7. Na, H. B.; Song, I. C.; Hyeon, T. Inorganic Nanoparticles for MRI Contrast Agents. *Adv. Mater.* **2009**, *21*, 2133–2148.
8. Häfeli, U. *Scientific and Clinical Applications of Magnetic Carriers*; Plenum Press: New York, 1997.
9. Dias, M. H. M.; Lauterbur, P. C. Ferromagnetic Particles as Contrast Agents for Magnetic Resonance Imaging of Liver and Spleen. *Magn. Reson. Med.* **1986**, *3*, 328–330.
10. Harisinghani, M. G.; Barentsz, J.; Hahn, P. F.; Deserno, W. M.; Tabatabaei, S.; van de Kaa, C. H.; de la Rosette, J.; Weissleder, R. Noninvasive Detection of Clinically Occult Lymph-Node Metastases in Prostate Cancer. *N. Engl. J. Med.* **2003**, *348*, 2491–2499.
11. Hyeon, T.; Lee, S. S.; Park, J.; Chung, Y.; Na, H. B. Synthesis of Highly Crystalline and Monodisperse Maghemite Nanocrystallites without a Size-Selection Process. *J. Am. Chem. Soc.* **2001**, *123*, 12798–12801.
12. Park, J.; An, K.; Hwang, Y.; Park, J.-G.; Noh, H.-J.; Kim, J.-Y.; Park, J.-H.; Hwang, N.-M.; Hyeon, T. Ultra-Large-Scale Syntheses of Monodisperse Nanocrystals. *Nat. Mater.* **2004**, *3*, 891–895.
13. Lee, J.-H.; Huh, Y.-M.; Jun, Y.-w.; Seo, J.-w.; Jang, J.-t.; Song, H.-T.; Kim, S.; Cho, E.-J.; Yoon, H.-G.; Suh, J.-S.; Cheon, J. Artificially Engineered Magnetic Nanoparticles for Ultrasensitive Molecular Imaging. *Nat. Med.* **2007**, *13*, 95–99.
14. Jun, Y.-w.; Lee, J.-H.; Cheon, J. Chemical Design of Nanoparticle Probes for High-Performance Magnetic Resonance Imaging. *Angew. Chem., Int. Ed.* **2008**, *47*, 5122–5135.
15. Na, H. B.; Lee, I. S.; Seo, H.; Park, Y. I.; Lee, J. H.; Kim, S.-W.; Hyeon, T. Versatile PEG-Derivatized Phosphine Oxide Ligands for Water-Dispersible Metal Oxide Nanocrystals. *Chem. Commun.* **2007**, 5167–5169.
16. Xu, C.; Xu, K.; Gu, H.; Zheng, R.; Liu, H.; Zhang, X.; Guo, Z.; Xu, B. Dopamine as a Robust Anchor To Immobilize Functional Molecules on the Iron Oxide Shell of Magnetic Nanoparticles. *J. Am. Chem. Soc.* **2004**, *126*, 9938–9939.
17. Xie, J.; Xu, C.; Xu, Z.; Hou, Y.; Young, K. L.; Wang, S. X.; Pourmand, N.; Sun, S. Linking Hydrophilic Macromolecules to Monodisperse Magnetite (Fe_3O_4) Nanoparticles *via* Trichloro-s-triazine. *Chem. Mater.* **2006**, *18*, 5401–5403.
18. Xie, J.; Xu, C.; Kohler, N.; Hou, Y.; Sun, S. Controlled PEGylation of Monodisperse Fe_3O_4 Nanoparticles for Reduced Non-specific Uptake by Macrophage Cells. *Adv. Mater.* **2007**, *19*, 3163–3166.
19. Long, M. J. C.; Pan, Y.; Lin, H.-C.; Hedstrom, L.; Xu, B. Cell Compatible Trimethoprim-Decorated Iron Oxide Nanoparticles Bind Dihydrofolate Reductase for Magnetically Modulating Focal Adhesion of Mammalian Cells. *J. Am. Chem. Soc.* **2011**, *133*, 10006–10009.
20. Lee, H.; Dellatore, S. M.; Miller, W. M.; Messersmith, P. B. Mussel-Inspired Surface Chemistry for Multifunctional Coatings. *Science* **2007**, *318*, 426–430.
21. Amstad, E.; Gillich, T.; Bilecka, I.; Textor, M.; Reimhult, E. Ultrastable Iron Oxide Nanoparticle Colloidal Suspensions Using Dispersants with Catechol-Derived Anchor Groups. *Nano Lett.* **2009**, *9*, 4042–4048.
22. Wu, H.; Zhu, H.; Zhuang, J.; Yang, S.; Liu, C.; Cao, Y. C. Water-Soluble Nanocrystals through Dual-Interaction Ligands. *Angew. Chem., Int. Ed.* **2008**, *47*, 3730–3734.
23. Bae, K. H.; Kim, Y. B.; Lee, Y.; Hwang, J.; Park, H.; Park, T. G. Bioinspired Synthesis and Characterization of Gadolinium-Labeled Magnetite Nanoparticles for Dual Contrast T1- and T2-Weighted Magnetic Resonance Imaging. *Bioconjugate Chem.* **2010**, *21*, 505–512.
24. Mei, B. C.; Susumu, K.; Medintz, I. L.; Delehanty, J. B.; Mountziaris, T. J.; Mattoussi, H. Modular Poly(ethylene glycol) Ligands for Biocompatible Semiconductor and Gold Nanocrystals with Extended pH and Ionic Stability. *J. Mater. Chem.* **2008**, *18*, 4949–4958.
25. Susumu, K.; Uyeda, H. T.; Medintz, I. L.; Pons, T.; Delehanty, J. B.; Mattoussi, H. Enhancing the Stability and Biological Functionalities of Quantum Dots *via* Compact Multifunctional Ligands. *J. Am. Chem. Soc.* **2007**, *129*, 13987–13996.
26. Stewart, M. H.; Susumu, K.; Mei, B. C.; Medintz, I. L.; Delehanty, J. B.; Blanco-Canosa, J. B.; Dawson, P. E.; Mattoussi, H. Multidentate Poly(ethylene glycol) Ligands Provide Colloidal Stability to Semiconductor and Metallic Nanocrystals in Extreme Conditions. *J. Am. Chem. Soc.* **2010**, *132*, 9804–9813.
27. Kim, S.-W.; Kim, S.; Tracy, J. B.; Jasanoff, A.; Bawendi, M. G. Phosphine Oxide Polymer for Water-Soluble Nanoparticles. *J. Am. Chem. Soc.* **2005**, *127*, 4556–4557.
28. Xu, Y.; Qin, Y.; Palchoudhury, S.; Bao, Y. Water-Soluble Iron Oxide Nanoparticles with High Stability and Selective Surface Functionality. *Langmuir* **2011**, *27*, 8990–8997.
29. Liu, W.; Greytak, A. B.; Lee, J.; Wong, C. R.; Park, J.; Marshall, L. F.; Jiang, W.; Curtin, P. N.; Ting, A. Y.; Nocera, D. G.; *et al.* Compact Biocompatible Quantum Dots *via* RAFT-Mediated Synthesis of Imidazole-Based Random Copolymer Ligand. *J. Am. Chem. Soc.* **2010**, *132*, 472–483.
30. Tahir, M. N.; Eberhardt, M.; Theato, P.; Faiß, S.; Janshoff, A.; Gorelik, T.; Kolb, U.; Tremel, W. Reactive Polymers: A Versatile Toolbox for the Immobilization of Functional Molecules on TiO_2 Nanoparticles. *Angew. Chem., Int. Ed.* **2006**, *45*, 908–912.
31. Shukoor, M. I.; Natalio, F.; Tahir, M. N.; Divekar, M.; Metz, N.; Therese, H. A.; Theato, P.; Ksenofontov, V.; Schröder, H. C.; Müller, W. E. G.; Tremel, W. Multifunctional Polymer-Derivatized γ-Fe_2O_3 Nanocrystals as a Methodology for the Biomagnetic Separation of Recombinant His-Tagged Proteins. *J. Magn. Magn. Mater.* **2008**, *320*, 2339–2344.
32. Shukoor, M. I.; Natalio, F.; Ksenofontov, V.; Tahir, M. N.; Eberhardt, M.; Theato, P.; Schröder, H. C.; Müller, W. E. G.; Tremel, W. Double-Stranded RNA Polyinosinic−Polycytidylic Acid Immobilized onto γ-Fe_2O_3 Nanoparticles by Using a Multifunctional Polymeric Linker. *Small* **2007**, *3*, 1374–1378.
33. Shukoor, M. I.; Natalio, F.; Metz, N.; Glube, N.; Tahir, M. N.; Therese, H. A.; Ksenofontov, V.; Theato, P.; Langguth, P.; Boissel, J.-P.; *et al.* dsRNA-Functionalized Multifunctional γ-Fe_2O_3 Nanocrystals: A Tool for Targeting Cell Surface Receptors. *Angew. Chem., Int. Ed.* **2008**, *47*, 4748–4752.
34. Tromsdorf, U. I.; Bigall, N. C.; Kaul, M. G.; Bruns, O. T.; Nikolic, M. S.; Mollwitz, B.; Sperling, R. A.; Reimer, R.; Hohenberg, H.; Parak, W. J.; *et al.* Size and Surface Effects on the MRI Relaxivity of Manganese Ferrite Nanoparticle Contrast Agents. *Nano Lett.* **2007**, *7*, 2422–2427.
35. Yi, D. K.; Lee, S. S.; Papaefthymiou, G. C.; Ying, J. Y. Nanoparticle Architectures Templated by SiO_2/Fe_2O_3 Nanocomposites. *Chem. Mater.* **2006**, *18*, 614–619.
36. Nasongkla, N.; Bey, E.; Ren, J.; Ai, H.; Khemtong, C.; Guthi, J. S.; Chin, S.-F.; Sherry, A. D.; Boothman, D. A.; Gao, J. Multifunctional Polymeric Micelles as Cancer-Targeted, MRI-Ultrasensitive Drug Delivery Systems. *Nano Lett.* **2006**, *6*, 2427–2430.
37. Kolb, H. C.; Finn, M. G.; Sharpless, K. B. Click Chemistry: Diverse Chemical Function from a Few Good Reactions. *Angew. Chem., Int. Ed.* **2001**, *40*, 2004–2021.
38. Han, H.-S.; Devaraj, N. K.; Lee, J.; Hilderbrand, S. A.; Weissleder, R.; Bawendi, M. G. Development of a Bioorthogonal and Highly Efficient Conjugation Method for Quantum Dots Using Tetrazine−Norbornene Cycloaddition. *J. Am. Chem. Soc.* **2010**, *132*, 7838–7839.
39. Bernardin, A.; Cazet, A.; Guyon, L.; Delannoy, P.; Vinet, F.; Bonnaffé, D.; Texier, I. Copper-Free Click Chemistry for Highly Luminescent Quantum Dot Conjugates: Application to *In Vivo* Metabolic Imaging. *Bioconjugate Chem.* **2010**, *21*, 583–588.
40. Haun, J. B.; Devaraj, N. K.; Marinelli, B. S.; Lee, H.; Weissleder, R. Probing Intracellular Biomarkers and Mediators of Cell Activation Using Nanosensors and Bioorthogonal Chemistry. *ACS Nano* **2011**, *5*, 3204–3213.

41. Hermanson, G. T. *Bioconjugate Techniques*, 2nd ed.; Elsevier Academic Press: Amsterdam, 2008.
42. Xing, Y.; Chaudry, Q.; Shen, C.; Kong, K. Y.; Zhau, H. E.; Chung, L. W.; Petros, J. A.; O'Regan, R. M.; Yezhelyev, M. V.; Simons, J. W.; *et al.* Bioconjugated Quantum Dots for Multiplexed and Quantitative Immunohistochemistry. *Nat. Protoc.* **2007**, *2*, 1152–1165.
43. Jung, C. W.; Jacobs, P. Physical and Chemical Properties of Superparamagnetic Iron Oxide MR Contrast Agents: Ferumoxides, Ferumoxtran, Ferumoxsil. *Magn. Reson. Imaging* **1995**, *13*, 661–674.
44. Rosenberg, J. T.; Kogot, J. M.; Lovingood, D. D.; Strouse, G. F.; Grant, S. C. Intracellular Bimodal Nanoparticles Based on Quantum Dots for High-Field MRI at 21.1 T. *Magn. Reson. Med.* **2010**, *64*, 871–882.
45. Pellegrino, T.; Manna, L.; Kudera, S.; Liedl, T.; Koktysh, D.; Rogach, A. L.; Keller, S.; Rädler, J.; Natile, G.; Parak, W. J. Hydrophobic Nanocrystals Coated with an Amphiphilic Polymer Shell: A General Route to Water Soluble Nanocrystals. *Nano Lett.* **2004**, *4*, 703–707.
46. LaConte, L. E. W.; Nitin, N.; Zurkiya, O.; Caruntu, D.; O'Connor, C. J.; Hu, X.; Bao, G. Coating Thickness of Magnetic Iron Oxide Nanoparticles Affects R2 Relaxivity. *J. Magn. Reson. Imaging* **2007**, *26*, 1634–1641.
47. Yu, W. W.; Chang, E.; Falkner, J. C.; Zhang, J.; Al-Somali, A. M.; Sayes, C. M.; Johns, J.; Drezek, R.; Colvin, V. L. Forming Biocompatible and Nonaggregated Nanocrystals in Water Using Amphiphilic Polymers. *J. Am. Chem. Soc.* **2007**, *129*, 2871–2879.